Acta Crystallographica Section D
Biological Crystallography
ISSN 0907-4449

Structure of murine Tcl1 at 2.5 Å resolution and implications for the TCL oncogene family

John M. Petock,[a] Ivan Y. Torshin,[a] Yuan-Fang Wang,[a] Garrett C. Du Bois,[b] Carlo M. Croce,[b] Robert W. Harrison[c] and Irene T. Weber[a]*

[a]Departments of Biology and Chemistry, Georgia State University, Atlanta, GA 30303, USA, [b]Departments of Microbiology and Immunology, Kimmel Cancer Center, Thomas Jefferson University, Philadelphia, PA 19107, USA, and [c]Department of Computer Science, Georgia State University, Atlanta, GA 30303, USA

Correspondence e-mail: iweber@gsu.edu

Received 25 March 2001
Accepted 13 August 2001

PDB Reference: murine Tcl1, 1jnp.

Tcl1 and Mtcp1, members of the Tcl1 family, are implicated in T-cell prolymphocytic leukemia. The crystal structure of a dimer of murine Tcl1 has been determined at 2.5 Å resolution with an *R* factor of 0.225. Murine Tcl1, human Tcl1 and Mtcp1 share very similar subunit structures, with RMS differences of 0.6 and 1.4 Å for C_α atoms, respectively, while the sequences share 50 and 36% identity, respectively. These structures fold into an eight-stranded β-barrel of unique topology and high internal symmetry of 1.1–1.3 Å for the two halves of human and murine Tcl1 and 1.7 Å for Mtcp1, despite the low 12–13% sequence identity. The molecular surfaces of all three structures showed a common planar region which is likely to be involved in protein–protein interactions.

1. Introduction

Human *TCL1*, *TCL1b* and *MTCP1* form a family of related oncogenes that are involved in the development of T-cell prolymphocytic leukemia and low-grade B-cell lymphomas (Stern *et al.*, 1993; Virgilio *et al.*, 1993). Although the physiological function of the *TCL1* family members is unknown, *TCL1* expression was found to occur primarily in developing B lymphocytes. *TCL1* is expressed in differentiated B cells with reactive and neoplastic conditions (Narducci *et al.*, 2000). Moreover, mice transgenic for *TCL1* and *MTCP1* were shown to develop mature T-cell leukemia (Gritti *et al.*, 1998; Virgilio *et al.*, 1998). Murine and human members of the *TCL1* family of oncogenes encode proteins of about 15 kDa that share 25–80% identical amino acids (Hallas *et al.*, 1999). However, there is no sequence similarity with other human genes. Recently, Tcl1, Tcl1b and Mtcp1 were shown to interact with the protein kinase Akt, which plays a key role in lymphoid proliferation and survival (Laine *et al.*, 2000; Pekarsky *et al.*, 2000).

The crystal structures of members of the *TCL1* family of oncoproteins are being studied in order to aid in understanding their biological function(s). Recently, we determined the crystal structure of human Mtcp1 (hMtcp1) that was refined to an *R* factor of 0.21 at 2.0 Å resolution (Fu *et al.*, 1998). The structure has a topologically unique eight-stranded β-barrel with a short helix between the fourth and fifth strands. Only the structure of the closely related Tcl1 shares the same β-barrel topology (Hoh *et al.*, 1998). Characterization of the role of *TCL1* family members in T-cell biology is complicated by the lack of sequence or structural similarities with other proteins of known function.

Here, the crystal structure of the murine Tcl1 (mTcl1) is reported and compared with the structures of human Tcl1 and Mtcp1. Murine Tcl1 consists of 116 amino-acid residues and shares 50% sequence identity with human Tcl1 (Hallas *et al.*,

1999). While hTcl1 crystallized with a monomer in the asymmetric unit of the $I222$ or $I2_12_12_1$ space group, mTcl1 crystallized with a dimer in the asymmetric unit of the $C2$ space group. The structures of murine and human Tcl1 were found to be very similar. Characterization of the murine Tcl1 structure will help to define common structural features and differences that could play key roles in the molecular interactions by which the *TCL1* family members influence T-cell biology.

2. Methods

2.1. Purification and crystallization of mTcl1

Murine Tcl1 was cloned in *Escherichia coli*, expressed and purified as described in Du Bois *et al.* (2000). The purified murine Tcl1 protein was concentrated to 5 mg ml^{-1} in 10 m*M* Tris buffer pH 7.5. The crystals were grown by vapor diffusion at room temperature using a well solution of 0.05 *M* sodium acetate and 0.1 *M* Tris pH 7.5; the hanging drops consisted of 1 µl each of protein and well solution. Small crystals grew within a week to dimensions of 0.01 × 0.01 × 0.03 mm. The largest crystals were branched and/or showed layers. Microseeding was performed after a 4 d equilibration without protein in vapor-diffusion trays using 0.05 *M* sodium acetate pH 3.9 and 1% 1-*O*-octyl-β-D-glucopyranoside in the wells and as drops on the cover slides. The sealed wells were then opened and microcrystals were added to the equilibrated drops on the cover slides with an additional 1 µl of mother liquor and 1 µl of a solution of 5 mg ml^{-1} protein in 0.1 *M* Tris buffer pH 7.5. Crystals were allowed to grow for five weeks before testing for diffraction.

2.2. Data collection and structure determination

X-ray diffraction data were collected on a Quantum 4 image-plate detector at beamline X12B of the National Synchrotron Light Source at Brookhaven National Laboratories. Only one murine Tcl1 crystal diffracted out of more than 30 crystals tested during the synchrotron trips. All other crystals were either too small or did not diffract. The data were processed with the *HKL* program package (Otwinowski & Minor, 1997). The structure solution was complicated owing to pseudo-merohedral twinning that generated a pseudo-$I222$ symmetry. Initially, the data were processed in the $I222$ space group, which was isomorphous to that observed for crystals of hTcl1 (Hoh *et al.*, 1998). The refinement was initiated using a homology model based on the hTcl1 structure that was constructed with the program *AMMP* (Harrison, 1993; Harrison *et al.*, 1995). The solution was confirmed by rotation and translation searches. This model did not refine properly. Because the initial indexing displayed higher metric symmetry, the data were reprocessed in the space group $C2$. The unit-cell parameters were $a = 89.320$, $b = 115.910$, $c = 37.870$ Å, $\alpha = 90.00$, $\beta = 115.11$, $\gamma = 90.00^\circ$. Merohedral twin tests were made using the Merohedral Crystal Twinning Server at the UCLA-DOE Laboratory of Structural Biology and Molecular Medicine UCLA website (http://www.doe-mbi.ucla.edu/services/Twinning). The results indicated that merohedral twinning was not present. The presence of higher metric symmetry was indicative of pseudo-merohedral twinning that cannot be detected by the merohedral twin servers.

Subsequent refinement was carried out with *SHELX*97 to handle crystal twinning (Sheldrick & Schneider, 1997; Herbst-Irmer & Sheldrick, 1998). A twin operator of [1 0 2, 0 −1 0, 0 0 −1] and a twin fraction of 0.49 were applied to transform the pseudo-*I*-centered orthorhombic cell into *C*-centered monoclinic. The refinement using the twin operator improved the *R* factor and eliminated much of the disorder in the electron-density maps. Manual refitting to the $2F_o - F_c$ and $F_o - F_c$ Fourier maps was performed using the program *TOM* on a Silicon Graphics Indigo2 computer (Cambillau *et al.*, 1987). The amino-terminal residues 1–7 and carboxy-terminal residues 109–116 were omitted from both subunits of the refined structure owing to the lack of electron density. The residues in the two subunits were numbered 1–116 and 201–316. The final refinement used diffraction data from 10.0 to 2.5 Å resolution and gave an *R* factor of 0.225 with an $R_{\rm free}$ of 0.236. The stereochemistry was analyzed with *PROCHECK* (Laskowski *et al.*, 1993). The murine Tcl1 coordinates are entry 1jnp in the PDB.

2.3. Comparison of mTcl1, hTcl1 and hMtcp1 crystal structures

The root-mean-square (RMS) differences were calculated for the superimposed pairs of C_α atoms of mTcl1, hTcl1 (PDB entry 1jsg) and hMtcp1 (PDB entry 1a1x) using the program *ALIGN* (Cohen, 1997). The internal symmetry was determined by superposition of the half-molecules of mTcl1, hTcl1 and hMtcp1. The half-molecules were defined as the first and last four β-strands of the eight-stranded β-barrel and excluded the short helix. The half-molecules consisted of residues 8–57 and 67–108 for the α-subunit of mTcl1 and the equivalent residues 208–257 and 267–308 for the β-subunit of mTcl1. The hTcl1 half-molecules consisted of residues 4–57 and 69–114; hMtcp1 was divided into residues 3–51 and 59–108. The figures of C_α structures were generated using the program *RasMol* (Sayle & Milner-White, 1995).

2.4. Analysis of surface models

Protein surfaces were generated with the program *WebLab ViewerLite* using a probe radius of 2.5 Å (Molecular Simulations Inc.). The solvent accessibility of residues was determined with the program *GETAREA* 1.1 (Fraczkiewicz & Braun, 1998). A probe radius of 2.5 Å was used for the calculation and the area/energy per residue was output. Any residue not identified in the output as solvent accessible or internal was checked in the program *WebLab ViewerLite*.

2.5. Sequence analysis of Tcl1 family members

The program *BLAST* was used to search for related proteins in the SwissProt and TrEMBL (translated EMBL) databases (Altschul *et al.*, 1990; Bairoch & Apweiler, 2000). Only proteins with alignments that spanned the whole sequence of the mTcl1 protein and had percentage identities

comparable to those within the Tcl1 family were considered. *PROSITE* was used to locate known functional sequence patterns in mTcl1, hTcl1 and hMtcp1 (Hofmann *et al.*, 1999).

3. Results and discussion

3.1. Refined crystal structure of mTcl1

The mTcl1 crystal structure was solved by molecular replacement using a model based on the hTcl1 structure; the data collection and refinement statistics are summarized in Table 1. The structure solution was complicated owing to pseudo-merohedral twinning that generated a pseudo-*I*222 symmetry. This type of twinning cannot be detected by the merohedral twin servers. Therefore, the structure was refined with *SHELX*97 to handle crystal twinning (Sheldrick & Schneider, 1997; Herbst-Irmer & Sheldrick, 1998). A twin operator of [1 0 2, 0 −1 0, 0 0 −1] and a twin fraction of 0.49 were applied to transform the pseudo-*I*-centered orthorhombic cell into *C*-centered monoclinic. The amino-terminal residues 1–7 and carboxy-terminal residues 109–116 were omitted from both subunits of the refined structure owing to the lack of electron density. The final structure consisted of two subunits of mTcl1 (each extending from residue 8 to 108) and 49 water molecules, and was refined to an *R* factor of 0.225 and an $R_{\rm free}$ of 0.236 using diffraction data to 2.5 Å resolution. The $2F_o - F_c$ electron-density map for three residues of the β-barrel is shown in Fig. 1. The electron-density map showed disorder or weak density in both subunits at the amino- and carboxy-termini and for the side chains of residues 54–56 and 66–68 in the loop regions before and after the short helix in both subunits. Consistent with the weak density, higher average *B* factors were observed in both subunits for the amino-terminal residues, residues 53–58 in the loop before the helical region and residues 98–101 in a turn between β-strands. Residues 67 and 68 in the loop following the helical region of the second subunit also had higher *B* factors. Val266 with disordered density was in a disallowed region of the Ramachandran plot. It is likely that the weak density and high *B* factors at surface loops is a consequence of the small crystal size, the twinning or working at the low-resolution limit recommended for *SHELX*97.

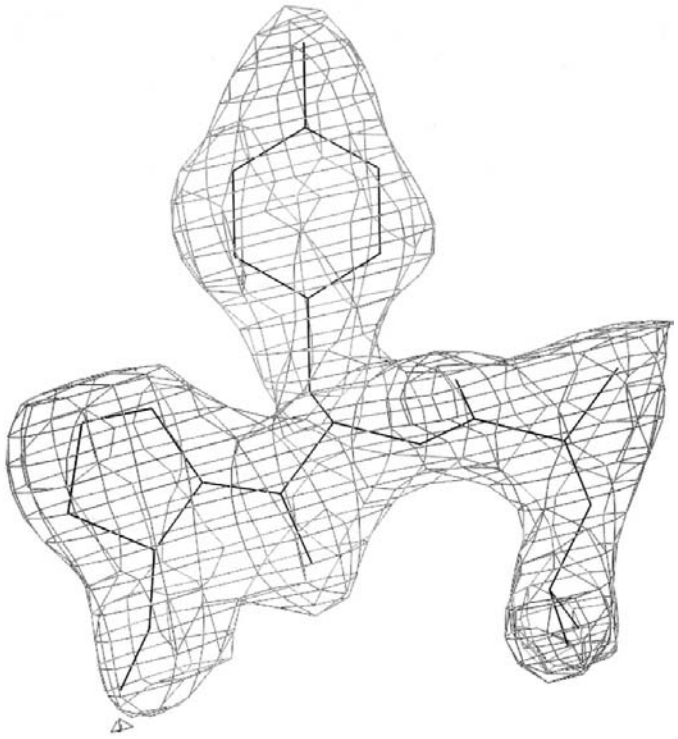

Figure 1
Electron-density map for residues Leu78, Tyr79 and Pro80 in the first subunit of mTcl1. The $2F_o - F_c$ map is contoured at a level of 1.0σ.

Table 1
Crystallographic data-collection and refinement statistics.

Resolution range (Å)	10.0–2.5
Space group	*C*2
Unit-cell parameters (Å, °)	a = 89.32, b = 115.91, c = 37.87, α = 90.00, β = 115.11, γ = 90.00
$R_{\rm merge}$	0.059
No. of reflections	
Total	11809
Unique	11019
Completeness (%)	
Overall	99.8
Last shell (2.59–2.50 Å)	99.5
$R_{\rm work}$ (%)	22.5
$R_{\rm free}$ (%)	23.6
No. of atoms	
Protein	1754
Solvent	49
B factors (Å^2)	
Main chain	36.8
Side chain	39.2
Solvent	32.0
$I/\sigma(I) > 3\sigma$ (%)	
Overall	87.1
Last shell	87.1
RMS deviation	
Bonds (Å)	0.019
Angles (°)	2.100

The two subunits in the asymmetric unit of mTcl1 were compared in order to evaluate the structural variability. The two subunits have very similar backbone structures, as shown in Fig. 2(*a*), and had an RMS deviation of 0.90 Å for 101 pairs of C_α atoms. The greatest structural variation occurs at the amino- and carboxy-termini; smaller differences are observed in several of the surface loops between β-strands and the long loop that contains the short helix.

3.2. Structural comparison of the Tcl1 family members

The three known structures in the Tcl1 family were compared in order to define common structural features and differences. Solution studies have shown that hTcl1 and mTcl1 form dimers, whereas hMtcp1 exists primarily as a monomer (Du Bois *et al.*, 1998, 2000). The crystal structure of mTcl1 was refined at 2.5 Å resolution to an *R* factor of 0.225 and hTcl1 was solved at 2.5 Å resolution with an *R* factor of 0.192, while hMtcp1 is the most accurate structure at 2.0 Å resolution with an *R* factor of 0.211. In the crystal, mTcl1 formed a dimer in the *C*2 space group, while hTcl1 was solved as a monomer in

the *I*222 space group and hMtcp1 crystals had a monomer in $P6_222$. Owing to the crystal twinning, it is not possible to define a unique set of crystal contacts, although one of the possible dimers of mTcl1 will be similar to the putative dimer of hTcl1. Interestingly, a Tcl1 trimer was observed in the study of the Tcl1 interaction with Akt (Laine *et al.*, 2000). Therefore, it is not clear what the physiological oligomer is and the different proteins may form different oligomers.

Overall, the crystal structures of all three proteins, mTcl1, hTcl1 and hMtcp1, are very similar with the exception of the amino- and carboxy-termini, as shown in Fig. 2(*b*). The eight-stranded β-barrel is structurally conserved, while the long surface loop, containing the short helix, shows more variation. The superimposed structures of murine and human Tcl1 showed RMS differences of 0.58 and 0.59 Å for the C_α atoms of the two subunits of mTcl1, respectively (Table 2). These RMS differences are similar to values of 0.4 Å reported for comparisons of different structures of identical proteins (Flores *et al.*, 1993). It is notable that the two subunits of mTcl1 have a larger RMS difference of 0.9 Å compared with 0.6 Å for comparison of hTcl1 and mTcl1, which share only 50% identical residues. Similar results were obtained for tumor necrosis factor-α, where crystallographic trimers of the wild type and mutant showed an RMS difference of 0.6 Å and pairs of subunits within the trimer had larger RMS differences of 0.8–1.1 Å (Reed *et al.*, 1997). In addition, hTcl1 and mTcl1 are structurally more conserved than has generally been observed for pairs of proteins sharing 50% sequence identity, where an average RMS difference of over 1.0 Å has been calculated (Flores *et al.*, 1993; Chothia & Lesk, 1986). Murine Tcl1 shares 36% sequence identity with human Mtcp1. Consistent with the sequence similarity, the Mtcp1 structure showed an RMS deviation of 1.44 and 1.52 Å for 97 of 101 pairs of C_α atoms in comparison with the two mTcl1 subunits, respectively. The larger differences were observed for the amino- and carboxy-termini, the loops before and after the helical turn and other surface loops between β-strands. Structural variability in the region of the short helix or helical turn was also observed in the NMR structure of human Mtcp1 (Guignard *et al.*, 2000).

Table 2
Structural differences among mTcl1, hTcl1 and hMtcp1.

RMS differences are given in Å with the percentage sequence identity in parentheses. 101 C_α atoms were compared for the two subunits of murine Tcl1, 100 C_α atoms for the comparison of murine and human Tcl1 and 97 for the comparison of murine Tcl1 and human Mtcp1. The internal symmetry involves 38 pairs of C_α atoms for each of the murine Tcl1 subunits and 42 C_α atoms for the analysis of human Tcl1 and Mtcp1.

	mTclb	hTcl1	hMtcp1	Internal symmetry
mTcla	0.90 (100%)	0.59 (50%)	1.44 (36%)	1.29 (12.2%)
mTclb	—	0.58 (50%)	1.52 (36%)	1.10 (12.2%)
hTcl1		—	1.49 (41%)	1.32 (13.3%)
hMtcp1			—	1.70 (13.3%)

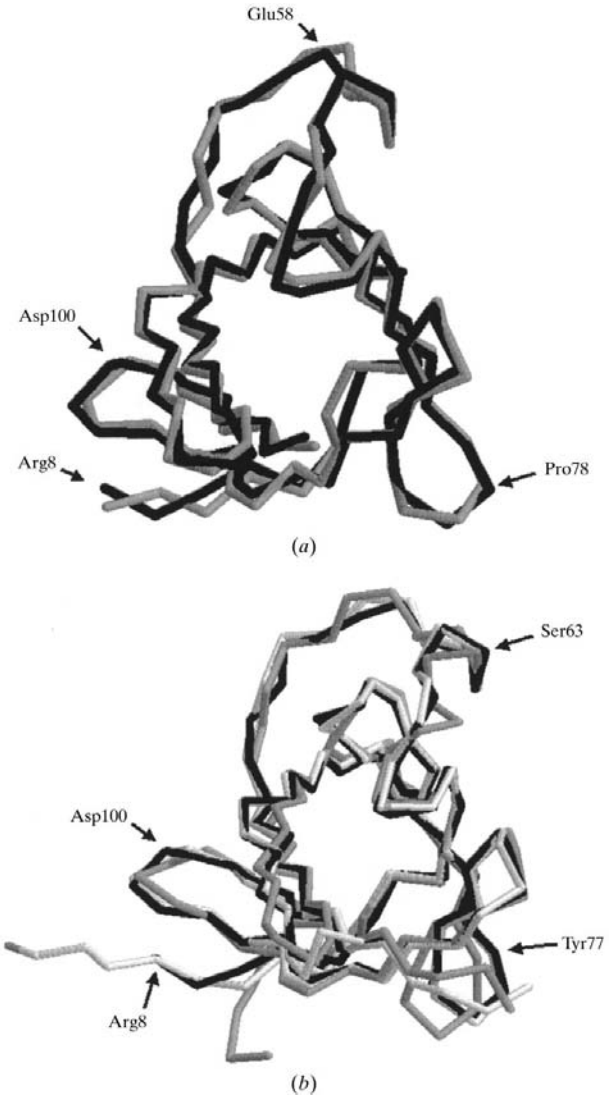

Figure 2
Structural comparisons of Tcl1 family members. (*a*) Superposition of C_α atoms of two subunits of murine Tcl1 (the two subunits are shown in black and gray). (*b*) Superimposed C_α atoms of mTcl1 (subunit 1 in black), hTcl1 (white) and hMtcp1 (gray).

Previously, the crystal structure of hTcl1 was shown to have an internal pseudo-twofold symmetry involving the two halves of the β-barrel structure (Hoh *et al.*, 1998). Similar internal symmetry is observed in the Mtcp1 and mTcl1 structures between the first four β-strands and the last four strands of the eight-stranded β-barrel. The two halves are separated by the short helix, which does not show the pseudo-symmetry. The sequences for the two halves and corresponding structural duplication are shown in Fig. 3. Outside the Tcl1 family, no other proteins were found to have significant sequence similarities to the half-motifs in *BLAST* searches. The internal structural symmetry was determined for each Tcl1 family member with the RMS deviation ranging from 1.10 to 1.70 Å for pairs of C_α atoms (Table 2). The human and murine Tcl1 showed a high degree of internal symmetry with RMS deviations of 1.1–1.3 Å, while Mtcp1 showed a slightly less symmetric structure with an RMS deviation of 1.7 Å. These low deviations suggest conservation of structure for each of the twofold halves, although their sequence identity is only 12–13% between the two half-structures. This structure conservation despite low sequence identity is consistent with the idea

```
                    --b---    --b--   ----b---     ---b----
mT matqrahrae tpahPnrLWi wekhvYlDEf rrsWlpvvik sne**kfqvi lrqedVtLGe
hT maecptlgea vtdhPdrLWa wekfvYlDEk qhaWlpltie ikdrlqlrvl lrredVvLGr
hM      maged vgapPdhLWv hqegiYrDEy qrtWvavvee ets**flrar vqqiqVpLGd
                  P  LW       Y DE     W                      V LG

       --a--        --b--    --b--  ------b----     ---b---
mT 59 amsPsqlvpy eLPlMWQLYP kdRYrscdSm yWqilyHikf rdVedmLLeL idsesnde
hT 61 pmtPtqigps lLPiMWQLYP dgRYrssdSs fWrlvyHiki dgVedmLLeL lpdd
hM 54 aarPshllts qLPlMWQLYP eeRYmdnnSr lWqiqhHlmv rgVqelLLkL lpdd
         P        LP MWQLYP   RY    S   W    H      V   LL L
```

(*a*)

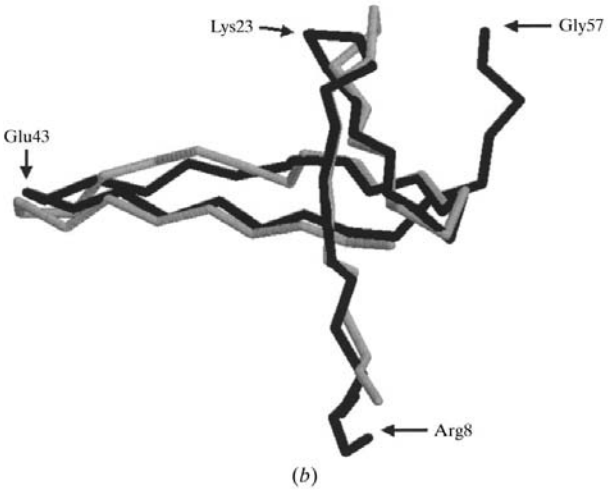

(*b*)

Figure 3
Internal pseudo-twofold symmetry in the Tcl1 protein family. (*a*) Sequence alignment for the two halves of murine Tcl1 (mT), human Tcl1 (hT) and human Mtcp1 (hM). (*b*) Superposition of C_α atoms in the two halves of the β-barrel in one subunit of mTcl1. Residues 8–57 and 67–108 corresponding to the two halves are colored black and gray, respectively.

that structure is much more conserved than sequence. Similar twofold duplication phenomenon was reported for structures with β/α-barrel scaffolds (Lang *et al.*, 2000).

3.3. Implications for function of Tcl1

The different members of the Tcl1 family of proteins, human Tcl1, Tcl1b and Mtcp1 and murine Tcl1, Tcl1b-Tcl1*b*5 and Mtcp1, share 25–80% amino-acid sequence identity (Hallas *et al.*, 1999). There is no significant sequence similarity with other known human genes. Since the physiological role of Tcl1 is not clear, we have searched the sequence databases for other proteins related to mTcl1 in order to obtain clues to its cellular function. Two proteins from *Arabidopsis thaliana* (mouse-ear cress) were found using the *BLAST*-related protein searches with the SwissProt and TrEMBL databases: T25B24.5 and T7N9.15/T7N9.20. The identities/positives values for T25B24.5 (SwissProt Q9SY90) and 7N9.15/T7N9.20 (SwissProt O04562) are 28/38% and 27/49%, respectively. The alignments span the whole sequence of the mTcl1 protein and the identity values are comparable with those of other Tcl1 proteins and better than those observed for mTcl1b3, which is the least similar to mTcl1 with 24/43% identities/positives. The *A. thaliana* protein T7N9.15 is mentioned in the PFAM database (PF00043) as being a member of the family of glutathione *S*-transferases (GSTs) (Bateman *et al.*, 1999). The Tcl1 proteins do not show any of the structural characteristics of enzymes. However, it is possible that mTcl1 shares similar functions to other GST family members proteins with no GST activity. The GST family includes eukaryotic elongation factors 1-γ and the HSP26 family of stress-related proteins, such as auxin-regulated proteins in plants and stringent starvation proteins in *E. coli*. Tcl1 may play a related role in normal lymphoid cell biology, since disruption of similar functions might lead to malignancies.

Recently, Tcl1, Tcl1b and Mtcp1 were shown to interact with the protein kinase Akt, which plays a key role in lymphoid proliferation and survival (Laine *et al.*, 2000; Pekarsky *et al.*, 2000). Tcl1 family members were shown to enhance the kinase activity of Akt as well as the transport of Akt to the nucleus. Such interactions could produce downstream events that lead to cell proliferation. Tcl1 was found to have the greatest interaction with the full-length Akt when compared with Mtcp1 and Tcl1b. In fact, the interaction of Tcl1 with Akt was over tenfold greater than that of Tcl1b and Mtcp1 based on β-galactosidase activity. Deletion analysis determined that the terminal residues 1–27 and 84–114 of Tcl1 were important, but not exclusive, for the binding to the PH domain of Akt. The termini show the largest structural variation on comparison of the crystal structures of Tcl1 and Mtcp1, although the overall fold is highly conserved. It is likely that differences in the surface residues of Tcl1 and Mtcp1, as well as conformational differences in the termini, contribute to the reported tenfold differences in interaction with Akt. Therefore, the sequences and molecular surfaces of mTcl1, hTcl1 and hMtcp1 were analyzed for potential sites of protein–protein interaction.

Comparison of the surface models of mTcl1, hTcl1 and hMtcp1 showed that there are three 'planar' regions in the mTcl1 molecule: the large broad surface near the N-terminus, the narrow surface between the C- and N-termini and a smaller surface near the C-terminus. The largest 'planar' surface was present in all three proteins (Figs. 4*a*–4*e*). This surface in mTcl1, hTcl1 and hMtcp1 is rather large (roughly 500 Å^2) and resembles the interacting surfaces of protein oligomers. The planar surface for mTcl1 includes residues 23–24, 37–43 and 52–69. In general, regions of protein–protein interactions in a set of homodimers were observed to involve planar interfaces with several clefts (Laskowski *et al.*, 1996). However, these large planar surfaces are distinct from the dimer-interface surfaces formed in the crystal structures of mTcl1, hTcl1 or hMtcp1. Each of the planar surfaces in Fig. 4 contains a series of 'knobs' and 'holes', which also suggests that the surfaces may be involved in protein–protein interactions. Hole/knob molecular surfaces used in 'geometric docking' were found to be an effective description of protein–

protein complexes (Norel *et al.*, 1994). All three proteins differ in the surface-charge distributions on these planar surfaces, which are critical for protein–protein recognition (Figs. 4*a*–4*e*), but the planar surface of each protein contains localized regions of negative charges separated from regions of positive charges. The negative and positive regions are positioned on the planar surfaces in different orientations in relation to the whole molecule, which suggests that the proteins cannot bind in an identical way to the same receptor and/or the proteins may bind to different receptors. In fact, the different members of the Tcl1 protein family may participate in quite different pathways by interacting with other proteins.

No phosphorylation of hTcl1, mTcl1 or hMtcp1 has been observed in the bacterially expressed proteins. However, since Tcl1 was shown to interact with the protein kinase Akt, the Tcl1 protein sequences were examined for other phosphorylation sites. Four potentially significant sequence patterns were found using *PROSITE*. The casein kinase II (CK2) phosphorylation site TLGE {PS00006: [ST]-X(2)-[DE]} was found in both murine Tcl1 (residues 55–58) and human Tcl1 (residues 6–9), but not in Mtcp1. CK2 is involved in cell proliferation and has the characteristic of not being regulated by calcium, cyclic AMP or other nucleotides. CK2 concentration is especially elevated in proliferating tissues, either normal or cancer-transformed (Pinna & Meggio, 1997). The potential CK2 phosphorylation site in mTcl1 is located in the surface loop leading to the short helix, which showed some disordered density and structural variation. It is possible that the disorder seen in the helical region of mTcl1 may arise from lack of phosphorylation; alternatively, it may be a consequence of the crystal lattice and the observed twinning. The potential CK2 phosphorylation sites were found in residues 6–9 (TLGE) near the amino-terminus of hTcl1, in residues 55–58 (TLGE) in the loop before the α-helix in mTcl1 and at the carboxy-terminal residues 113–116 (SNDE) of mTcl1. These residues are located on surface-accessible regions of the structures and potentially accessible for phosphorylation. As previously mentioned, a narrow planar surface is present between the amino- and carboxy-termini in both murine and human Tcl1. Thus, potential protein–protein interactions through this narrow planar surface may be modulated owing to CK2 phosphorylation. A tyrosine kinase phosphorylation site RSADSMY {PS00007: [Rk]-X(3)-[DE]-X(2)-Y and [Rk]-X(2)-[DE]-X(3)-Y} was found in mTcl1 residues 83–89; however, this sequence is not conserved in the other Tcl1 family members. No potential phosphorylation sites were found in Mtcp1. If the non-conserved phosphorylation sequences in mTcl1 and hTcl1 are functional then it is likely that the proteins are regulated in different ways.

The newly determined crystal structure of murine Tcl1 has been compared

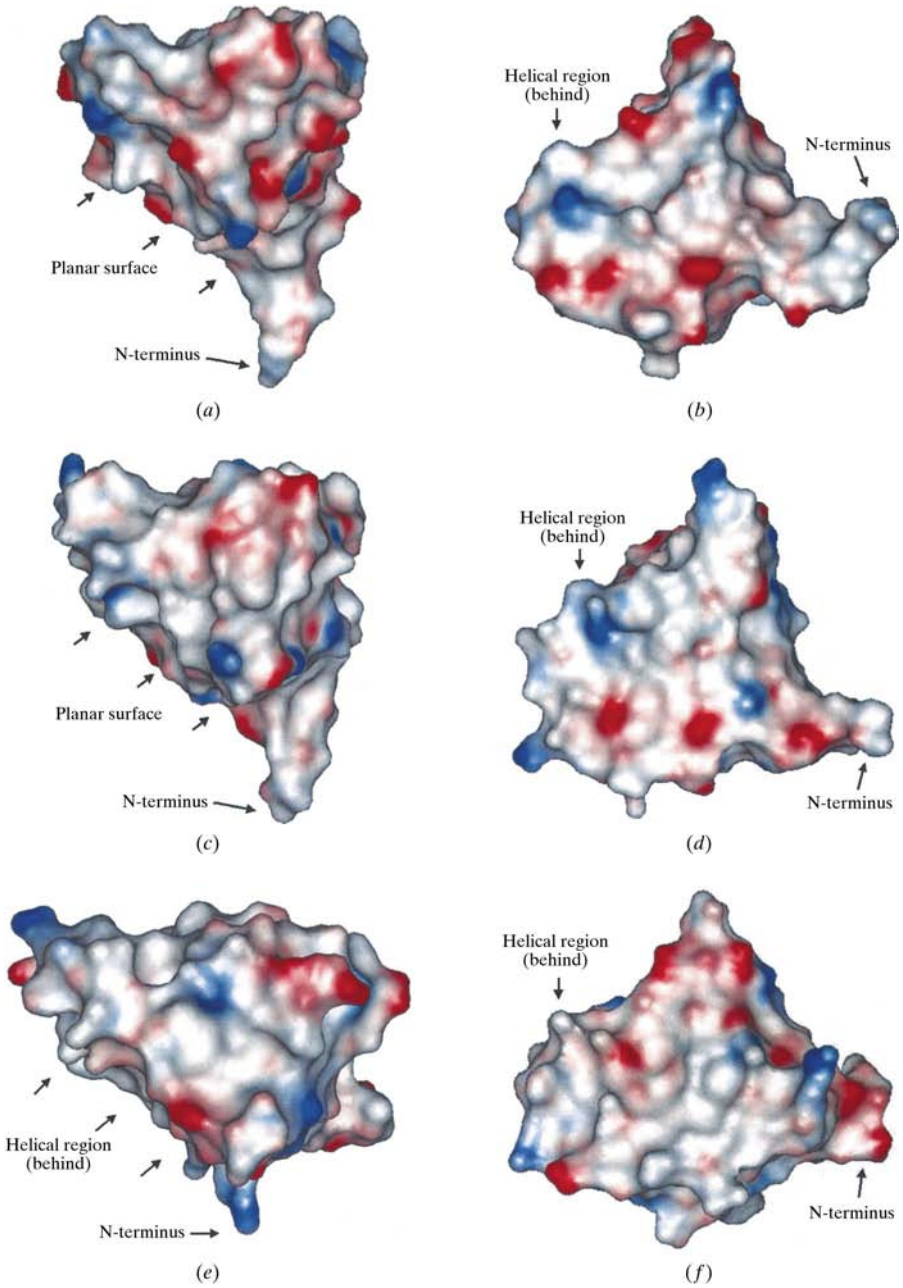

Figure 4
Molecular-surface analysis. The extensive planar surface is shown in the same orientation for the subunits of mTcl1, hTcl1 and hMtcp1. Protein surfaces were generated with the program *WebLab ViewerLite* using a probe radius of 2.5 Å (Molecular Simulations Inc.). Regions of negative electrostatic potential are colored red and positive regions are blue. (*a*) mTcl1, side view; (*b*) mTcl1, front view; (*c*) hTcl1, side view; (*d*) hTcl1, front view; (*e*) hMtcp1, side view; (*f*) hMtcp1, front view.

with the crystal structures of human Tcl1 and Mtcp1, other members of the Tcl1 family. The crystal structure of murine Tcl1 contains two subunits; however, the dimer is not equivalent to that of human Tcl1. The three different proteins share very similar structures of an eight-stranded β-barrel with a long surface loop containing a short helical region that separates the two four-stranded pseudo-symmetric 'half-barrel' structures. Analysis of the sequences and molecular surfaces of the three proteins has been used to provide clues to potential sites for protein–protein interactions and the physiological function. Murine Tcl1, human Tcl1 and Mtcp1 subunits share a similar large planar surface that resembles other known protein–protein interfaces. However, the charge distribution over these planar surfaces differs among the proteins, which leads to the conclusion that mTcl1, hTcl1 and hMtcp1 cannot interact with the same proteins in the same manner. Potentially accessible phosphorylation sites were located in different regions of human and murine Tcl1, suggesting that the proteins may be regulated in different ways. Therefore, although the Tcl1 proteins share similar structures, they are likely to interact with different cellular proteins.

We thank Dr Bhuvaneshwari Mahalingam for help with synchrotron data collection and Drs George Sheldrick and Regine Herbst-Irmer for advice on the crystal twinning. The diffraction data were collected at beamline X12B of the National Synchrotron Light Source, Brookhaven National Laboratory. This research was supported in part by the Elsa U. Pardee Foundation and the National Cancer Institute grant CA76259.

References

Altschul, S. F., Gish, W., Miller, W., Myers, E. W. & Lipman, D. J. (1990). *J. Mol. Biol.* **215**, 403–410.
Bairoch, A. & Apweiler, R. (2000). *Nucleic Acids Res.* **28**, 45–48.
Bateman, A., Birney, E., Durbin, R., Eddy, S. R., Finn, R. D. & Sonnhammer, E. L. (1999). *Nucleic Acids Res.* **27**, 260–262.
Cambillau, C. M., Oatley, S. J., Bush, B. L., Jones, T. A., Pflugrath, J. W., Saper, M. A. & Sack, J. S. (1987). *TOM – Molecular Graphics Program for the IRIS Version* 2.4. http://www.imb-jena.de/www_sbx/tom.html.
Chothia, C. & Lesk, A. M. (1986). *EMBO J.* **5**, 823–826.
Cohen, G. E. (1997). *J. Appl. Cryst.* **30**, 1160–1161.
Du Bois, G. C., Song, S. P., Kulikovskaya, I., Rothstein, J. L., Germann, M. W. & Croce, C. M. (2000). *Protein Expr. Purif.* **18**, 277–285.
Du Bois, G. C., Song, S. P., Kulikovskaya, I., Virgilio, L., Varnum, J., Germann, M. W. & Croce, C. M. (1998). *Protein Expr. Purif.* **12**, 215–225.
Flores, T. P., Orengo, C. A., Moss, D. S. & Thornton, J. M. (1993). *Protein Sci.* **2**, 1811–1826.
Fraczkiewicz, R. & Braun, W. (1998). *J. Comput. Chem.* **19**, 319–333.
Fu, Z. Q., Du Bois, G. C., Song, S. P., Kulikovskaya, I., Virigilio, L., Croce, C. M., Weber, I. T. & Harrison, R. W. (1998). *Proc. Natl Acad. Sci. USA*, **95**, 3413–3418.
Gritti, C., Dastot, H., Soulier, J., Janin, A., Daniel, M. T., Madani, A., Grimber, G., Briand, P., Sigaux, F. & Stern, M. H. (1998). *Blood*, **92**, 368–373.
Guignard, L., Padilla, A., Mispelter, J., Yang, Y. S., Stern, M. H., Lhoste, J. M. & Roumestand, C. (2000). *J. Biol. NMR*, **17**, 215–230.
Hallas, C., Pekarsky, Y., Itoyama, T., Varnum., J., Bichi., R., Rothstein, J. L. & Croce, C. M. (1999). *Proc. Natl Acad. Sci. USA*, **96**, 14418–14423.
Harrison, R. W. (1993). *J. Comput. Chem.* **14**, 1112–1122.
Harrison, R. W., Chatterjee, D. & Weber, I. T. (1995). *Proteins Struct. Funct. Genet.* **23**, 463–471.
Herbst-Irmer, R. & Sheldrick, G. M. (1998). *Acta Cryst.* B**54**, 443–449.
Hofmann, K., Bucher, P., Falquet, L. & Bairoch, A. (1999). *Nucleic Acids Res.* **27**, 215–219.
Hoh, F., Yang, Y. S., Guignard, L., Padilla, A., Stern, M. H., Lhoste, J. M. & van Tilbeurgh, H. (1998). *Structure*, **6**, 147–155.
Laine, J., Künstle, G., Obata, T., Sha, M. & Noguchi, M. (2000). *Mol. Cell*, **6**, 395–407.
Lang, D., Thoma, R., Henn-Sax, M., Sterner, R. & Wilmanns, M. (2000). *Science*, **289**, 1546–1550.
Laskowski, R. A., Luscombe, N. M., Swindells, M. B. & Thornton, J. M. (1996). *Protein Sci.* **12**, 2438–2452.
Laskowski, R. A., MacArthur, M. W., Moss, D. S. & Thornton, J. (1993). *J. Appl. Cryst.* **26**, 283–291.
Narducci, M. G., Pescarmona, E., Gignoretti, S., Lavinia, A. M., Remotti, D., Scala, E., Baroni, C. D., Stoppacciarro, A., Croce, C. M. & Russo, G. (2000). *Cancer Res.* **60**, 2095–2100.
Norel, R., Lin, S. L., Wolfson, H. J. & Nussinov, R. (1994). *Biopolymers*, **7**, 933–940.
Otwinowski, Z. & Minor, W. (1997). *Methods Enzymol.* **276**, 307–326.
Pekarsky, Y., Koval, A., Hallas, C., Bichi, R., Tresini, M., Malstrom, S., Russo, G., Tsichlis, P. & Croce, C. M. (2000). *Proc. Natl Acad. Sci. USA*, **97**, 3028–3033.
Pinna, L. A., & Meggio, F. (1997). *Prog. Cell Cycle Res.* **3**, 77–97.
Reed, C., Fu, Z.-Q., Wu, J., Xue, Y.-N., Harrison, R. W., Chen, M.-J. & Weber, I. T. (1997). *Protein Eng.* **10**, 1101–1107.
Sayle, R. A. & Milner-White, J. E. (1995). *Trends Biochem. Sci.* **20**, 374.
Sheldrick, G. M. & Schneider, T. R. (1997). *Methods Enzymol.* **277**, 319–343.
Stern, M. H., Soulier, J., Rosenzwajg, M., Nakahara, K., Canki-Klain, N., Aurias, A., Sigaux, F., Kirsch, I. R. (1993). *Oncogene*, **8**, 2475–2483.
Virgilio, L., Isobe, M., Narducci, M. G., Carotenuto, P., Camerini, B., Kurosawa, N., Abbas-ar-Rushdi, Croce, C. M. & Russo, G. (1993). *Proc. Natl Acad. Sci. USA*, **90**, 9275–9279.
Virgilio, L., Lazzeri, C., Bichi, R., Nibu, K. I., Narducci, M. G., Russo, G., Rothstein, J. & Croce, M. (1998). *Proc. Natl Acad. Sci. USA*, **95**, 3885–3889.